ESKİŞEHİR TECHNICAL UNIVERSITY JOURNAL OF SCIENCE AND TECHNOLOGY
A- APPLIED SCIENCES AND ENGINEERING

2022, 23(4), pp. 233-243, DOI: 10.18038/estubtda.899963

CONTRIBITION OF MICRO-SILICA AND NANO-MONTMORILLONITE REINFORCEMENTS ON THE MECHANICAL PROPERTIES OF UV-CURABLE THERMOSET RESIN

Ayşe Çağıl KANDEMİR [1,*], Arda BAYTAROĞLU [1]

[1] Mechanical Engineering, Faculty of Engineering, TED University, Ankara, Turkey

ABSTRACT

UV-curable thermoset resins had been utilized in organic coating industry because of their benefits over conventional adhesives like fast curing, less energy consumption and equipment. In this article, the effects of micro and nano-scaled reinforcements on the mechanical properties of a UV-curable thermoset resin were investigated. The reinforcements are chosen to be nano-scaled Montmorillonite (MMT) and micro-scaled Silica (SiO_2). The reason for this choice is that the aforementioned particles are non-toxic, low-cost and in the case of MMT; abundant in nature. According to our knowledge, there is no study on the synergistic effects of those two additives in thermoset resins.

The instrumented microindentation test results reveal that maximum improvement on hardness (288%) was achieved by single addition of MMT thanks to the well-distributed silicate layers. Conversely, SiO_2 addition diminished both strength (-51%) and modulus (-68%) drastically which is attributed to the possible poor dispersion and weak surface attraction. On the other hand, when those additives were utilized together, the property improvements namely; hardness and modulus are observed to be in between of single addition of either additive. It is suggested that SiO_2 contribution does not disturb intercalated/exfoliated-MMT structure and similarly by simultaneous MMT reinforcement, quality of SiO_2 dispersion is not affected. It is concluded that one benefit of these SiO_2-MMT combinations over single MMT reinforcement could be related to plasticity since they result in less plasticity reduction of -22%-27% compared to MMT (-43%) with the further benefit of higher hardness improvement (+66%) than bare SiO_2 addition (-51%).

Keywords: Clay, Silicas, Composites, Film, Thermoset

1. INTRODUCTION

UV-curable thermoset resins had been utilized in organic coating industry because of their advantages like fast curing, less energy consumption and equipment in comparison with conventional curing methods. Crosslinking density of the thermoset resins could be increased to improve strength, though it leads to brittleness. The alternative for this is utilizing reinforcements by composite approach. In this study, nano-scaled Montmorillonite (MMT) and micro-scaled silica (SiO_2) were focused as they are non-toxic, low-cost and in the case of MMT; abundant in nature.

Studies show that both nano and micro-scaled silica particles either improve or diminish strength of thermoset matrices depending on mainly their surface compatibility [1– 3]. For instance, in the study of Ahmad et al. [1] nano-silica addition to epoxy resin diminished both strength and elastic modulus while in the study of Li et al. [2] both properties were improved thanks to the surface compatibility of composite constituents. In the study of Meng et. al., micro and nano silica reinforcements were utilized to toughen epoxy [3]. The study yielded that nano-silica could much more efficiently toughen the ductile epoxy matrix such that 738% and 60% improvements were achieved for 4 wt% nano and micro-silicas, respectively. This behavior is attributed to the higher surface area and smaller particle-particle distance of nano-silica.

*Corresponding Author: cagil.kandemir@tedu.edu.tr
Received: 19.03.2021 Published: 29.12.2022

There are many studies focusing on Montmorillonite (MMT) based adhesive composites [4– 9]. Silicate layers have very high aspect ratio (could be as high as 500) enabling effective stress transfer from matrix to MMT. In order to achieve this, intercalation/exfoliation level of them play a significant role. For instance, in the study of Menezes et al. [9] highest improvement in both strength and modulus of a dental adhesive is achieved by just 0.2 wt% exfoliated MMT addition while those properties declined with further MMT addition. This shows that dispersion quality and the exfoliation level are key parameters as increase in MMT concentration causes agglomeration. In the study of Alsagayar et al. [5] when MMT loading in epoxy resin exceeds 1 wt% both strength and modulus diminish because of poor dispersion pointing out the necessity of exfoliation.

The main aim of this study to investigate influence of nano-scaled MMT and micro-scaled SiO_2 on the mechanical properties of UV-curable thermoset resin. The reason for the choice of these particles is that they are non-toxic, low-cost and in the case of MMT; abundant in nature. According to our knowledge, there is no study on the mutual effects of those two particles in thermoset resins. The films of the composites were produced either on glass slides or as free-standing films. Dispersion of the particles was observed by XRD and FTIR analyses while mechanical behavior was tested via instrumented microindentation. In this study, plasticity was utilized to comment on the underlying deformation mechanisms. The outcomes were interpreted in terms of the size, shape, surface compatibility and dispersion of the particles.

2. EXPERIMENTAL

2.1. Materials

UV-curable thermoset resin is chosen as the polymer matrix having the commercial name of NOA 61 (Norland Optics). NOA 61 is not composed of volatile components, which is beneficial for long-term stability. As for the reinforcements, unmodified amorphous silica particles (1 μm) and organically modified- nanoclay (35-45% dimethyl dialkyl (C14-C18) amine modified Montmorillonite) were chosen for micro-scaled/ spherical and nano-scaled/ layered reinforcements, respectively. Silica particles and nanoclay were purchased from Sigma Aldrich and Nanografi (Ankara, Turkey), respectively.

2.2. Production of Composites

Firstly, an appropriate solvent was sought since the solvent-mixing method was going to be applied for composite production. The solvents: deionized water, ethanol and tetrahydrofuran were tried. Inspection by naked eye revealed that tetrahydrofuran is the most appropriate solvent for the particular UV-curable resin. Ethanol and deionized water usage as solvent resulted in more agglomerated morphology which was visible to naked eye while via tetrahydrofuran solvent, agglomeration was not observed. Similar results were also found in the previous study of the author with a comparable UV-curable resin [10–11].

The composite production consists of three main parts. Firstly, NOA 61 was dissolved in the solvent which is chosen to be tetrahydrofuran in magnetic stirrer for two hours. Secondly, reinforcements were induced to the solution and mixed for four hours by magnetic stirrer. Lastly, the solution was poured in either of the followings: to a Teflon plate or on a glass slide for XRD/ FTIR analyses, or microindentation test, respectively. Subsequently, UV-curing (365 nm-wavelength) was applied. The composite coatings which were exposed to micro-indentation test are shown in Figure 1 while standalone films taken from Teflon molds are shown in Figure 4. Designation and the weight percentages of composite constituents are shown in Table 1.

Table 1. Designation of the composite films and the weight percentages of their constituents.

	Polymer	**Polymer_ MMT**	**Polymer_MMT_ 2**	**Polymer_ SiO**	**Polymer_SiO_ MMT**	**Polymer_SiO_ MMT_2**
MMT	-	1 wt%	5 wt%		1 wt%	0.5 wt%
SiO_2	-	-	-	1 wt%	1 wt%	0.5 wt%

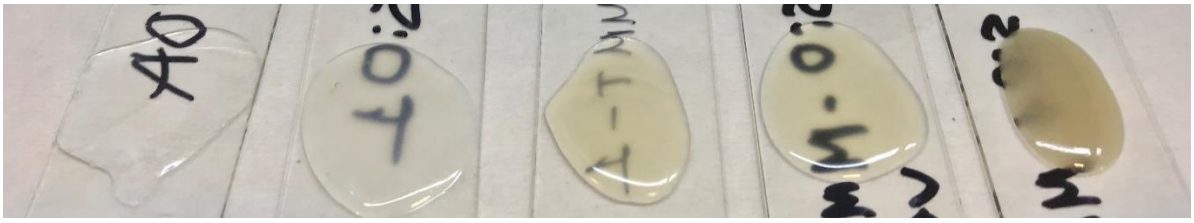

(a) **(b)** **(c)** **(d)** **(e)**

Figure 1. Polymer and composite coatings on glass slides which subsequently exposed to Micro-indentation test are shown: a)Polymer b) Polymer_SiO c) Polymer_MMT d) Polymer_SiO_MMT_2 e) Polymer_SiO_MMT.

2.3. X- ray Diffraction Analysis

To evaluate dispersity and the intercalation/exfoliation of Montmorrilonite silicate layers in thermoset resin, wide angle X- ray diffraction analysis (XRD) (Rigaku Ultima-IV, CuKa 40 kV, 40 mA) was conducted under a continuous scanning range of 2–10º in Middle East Technical University Central Laboratory.

2.4. FTIR Spectroscopy

Fourier Transformed Infrared Spectroscopy (FTIR) was accomplished in Middle East Technical University Central Laboratory (Bruker IFS 66/S) in order to confirm the surface compatibility of matrix with the reinforcements.

2.4. Mechanical Characterization

Instrumented micro-indentation test with Vickers indenter was conducted in Middle East Technical University Central Laboratory (CSM Instruments). The tests were accomplished by a maximum force of 5 mN. Hardness and Elastic Modulus values were calculated by using Oliver-Pharr method [25-26]. The equations used for the calculation of elastic modulus are revealed in (1) and (2). S is the slope of unloading curve, A is the contact area, β is the dimensionless parameter close to unity, E_{eff} is the effective modulus combining moduli of the indenter and the sample. υ, υ_i, E and Ei are Possion's ratio of sample, Possion's ratio of indenter, elastic modulus of sample and elastic modulus of indenter, respectively. The plasticity was measured by the ratio of the plastic work to the total work of force-indentation depth curves.

$$S = \beta \frac{2}{\sqrt{\pi}} Eeff\sqrt{A} \tag{1}$$

$$\frac{1}{Eeff} = \frac{1-v^2}{E} + \frac{1-vi^2}{Ei} \tag{2}$$

3. RESULTS

The results of XRD are represented in Figure 2. Sharp peaks does not exist in the patterns of Polymer, Polymer_MMT, Polymer_MMT_SiO and Polymer_MMT_SiO_2. In contrary, two distinctive peaks were found in Polymer_MMT which correspond to 2θ degress of 2.510º and 4.935º. FTIR Spectroscopy was accomplished for three samples; Polymer, Polymer_MMT and Polymer_SiO (Figure 3-4). There are no major peak differences in all of the FTIR patterns. However, in the case of Polymer_SiO; at the wave numbers of 522 cm^{-1} and 462 cm^{-1}there are two distinctive peaks differs from Polymer.

Micro-indentation test was applied in order to measure mechanical properties of the samples (Table 2, Figure 5). Hardness and Elastic Modulus values were calculated by using Oliver Pharr method [25-26]. Hardness of the samples were found to be 169.608±2.190, 657.394±116.394, 84.618±11.015, 282.166±15.00 and 126.906±23.705 for Polymer, Polymer_MMT, Polymer_SiO, Polymer_SiO_MMT and Polymer_SiO_MMT_2, respectively. While for the same samples elastic moduli were revealed to be 6.834±1.314, 7.613±0.337, 2.225±0.213, 5.022±0.567 and 3.288±0.432, respectively.

4. DISCUSSION

4.1. Interaction Between Matrix and the Reinforcements

The exact formula of the polymer (commercial name: NOA 61) is unknown. However, previous studies revealed that the main constituents of which are; mercapto-ester and tetrahydrofurfuryl metachrylate. The study of Castiriota et al. showed that main curing reaction occurs by the interaction of thiol group (R-SH) and C=C [12]. Consequently, the fully cured polymer should not have C=C and S-H bond. FTIR spectra of the polymer in Figure 3 does not show the specific peak of aliphatic C=C (1638 cm^{-1}) pointing out the efficient crosslinking while there exists a weak peak of S-H at 2570 cm^{-1}.

Insertion of 1 wt% of either SiO_2 or MMT neither increased the intensity of S-H peak nor led to formation of C=C peak (Figure 3). This could be interpreted as crosslinking density was not affected by the reinforcements. The peaks of Polymer_SiO are identical with the pristine polymer while two additional peaks (462 and 522 cm^{-1}) were observed for Polymer_MMT (Figure 3, Figure 4). This reveals that there is no considerable chemical interaction of polymer chains with unmodified-SiO_2 surface. On the contrary, interaction exists between MMT and the matrix indicating that organically-modified MMT surface is compatible with the polymer chains. This is also further confirmed by the XRD Analysis.

Figure 2 reveals XRD outcomes showing that addition of 5 wt% MMT in the polymer matrix (Polymer_MMT_2) resulted in two peaks. Since there were no visible peaks in the XRD pattern of the polymer (because of its amorphous structure), it can be said that these two peaks are directly due to MMT addition. The first sharp peak at $2\theta = 2.510°$ coincides to the interlayer spacing (d-spacing) of 3.517 nm. The calculated value of initial interlayer spacing of MMT is 2.658 nm. Looking at this result, increase of inter-gallery distance to 3.517 nm from 2.658 nm reveals that silicate layers are firmly intercalated by the molecular chains of the polymer. The second peak that occurred at $2\theta = 4.935°$ can be due to the second-order reflection since the calculations with the Bragg's Law indicates an interlayer spacing of 3.577 nm. Moreover, decreasing MMT loading to 1 wt% (Polymer_MMT) diminished all visible XRD Peaks which could be either interpreted as exfoliated microstructure was achieved with this particular composition or this could be resulted from decreased intensity. Nevertheless, this particular composition should have at least intercalated morphology with possible exfoliation as the FTIR (Figure 4) characterization reveals chemical interaction between nanocomposite constituents. It is also well-known from the literature that as the nanoclay concentration decreases, intercalation/exfoliation level increases. Because of these revelations, only Polymer_MMT was exposed to further mechanical test owing to its suggested better dispersion than Polymer_MMT_2.

Additionally, when equal amounts of MMT and SiO_2 (either 1 wt% or 0.5 wt%) were added together, similar to Polymer_MMT, sharp XRD peaks were not observed in their corresponding curves (Figure 2) suggesting that high dispersion quality was preserved.

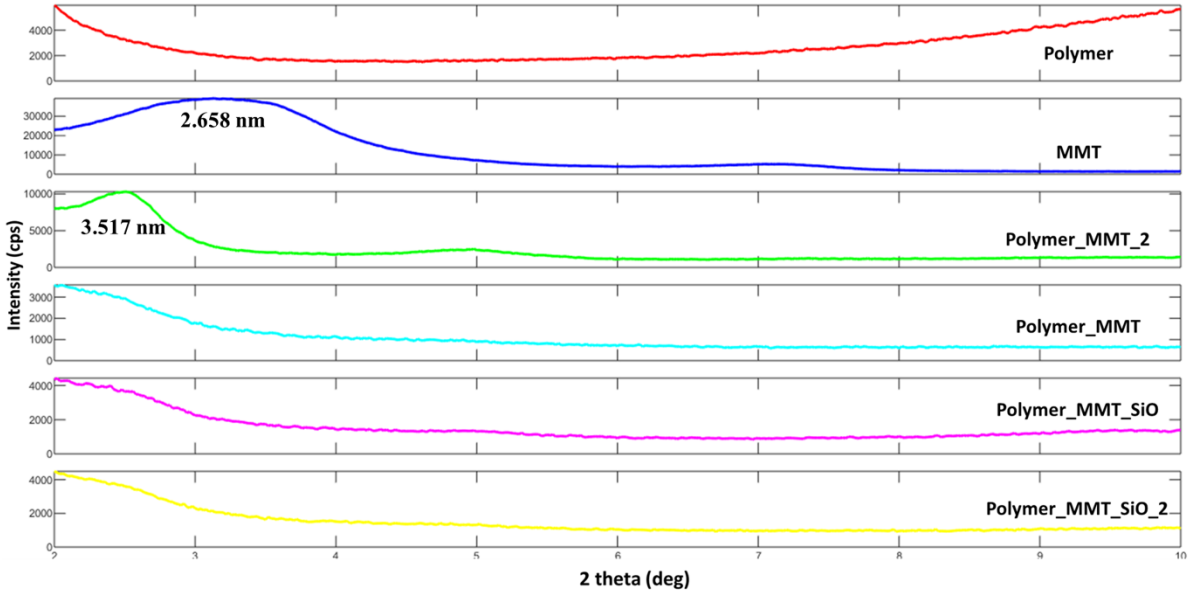

Figure 2. XRD outcomes of the polymer and composites are shown.

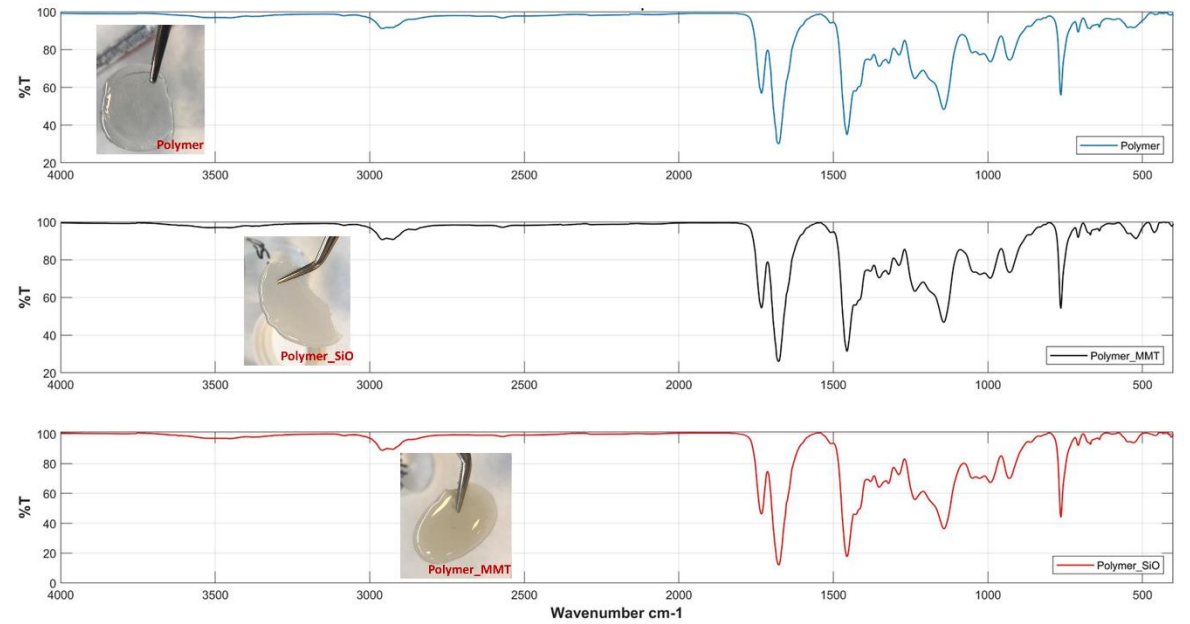

Figure 3. FTIR spectra of the polymer and composites.

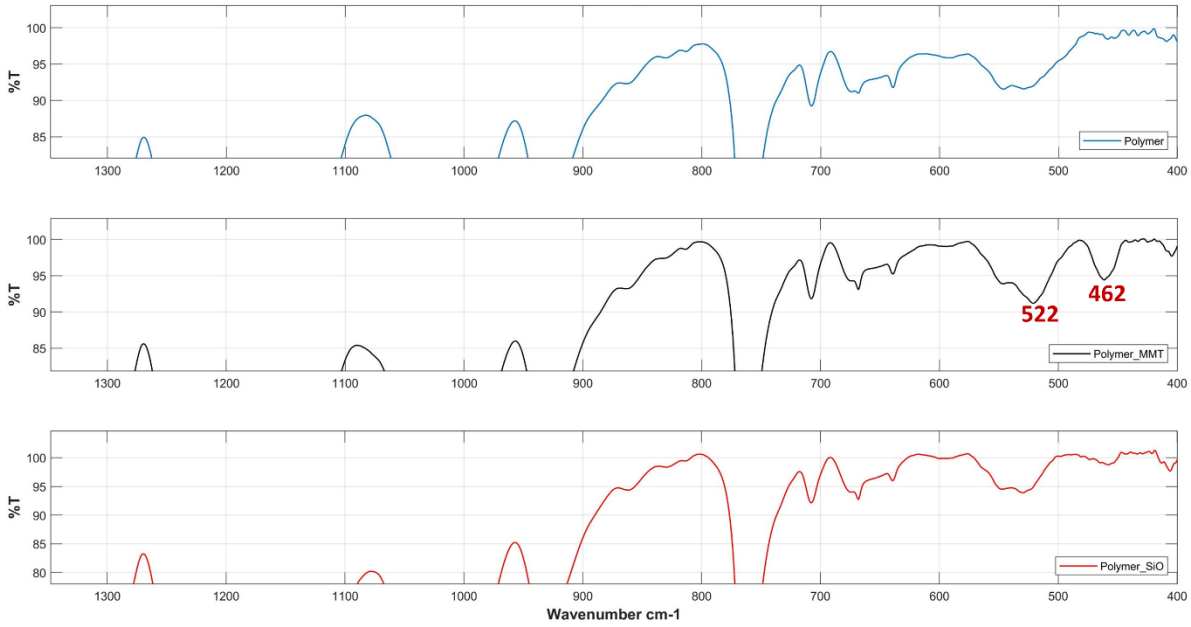

Figure 4. FTIR spectra concentrated on 400-1350 cm^{-1}.

4.2. Mechanical Properties

Micro-indentation test (Table 2, Figure 5) results reveal that the pristine polymer without any reinforcing agent has higher hardness (169.6 MPa) and elastic modulus (6.8 GPa) in comparison with its tensile test outcomes (tensile strength: 20 MPa, tensile modulus: 1 GPa; which are taken from the data sheet [13]). It should be noted that the results were obtained from a 'compressive test'. Generally, for most materials, hardness is 3-4 times higher than the tensile strength. Nevertheless, the results of this study indicate more than 8-fold overshoot of the strength. This could be attributed to the 'chain confinement effect' leading to chain entanglement in nm-scale.

It is seen that both polymer and composites are prone to creep throughout indentation because of their viscoelastic nature. Creep is basically increase in indentation depth right away after unloading, even though the applied force is diminishing, [14]. Creep might result in a 'nose effect' on unloading curve which disturbs elastic modulus measurement [14– 18]. It is suggested [17] to hold on at maximum load for a time period to reduce the creep effect, which was also conducted in this study, by holding all samples for 30 seconds to release viscoelasticity effect (Figure 5 a).

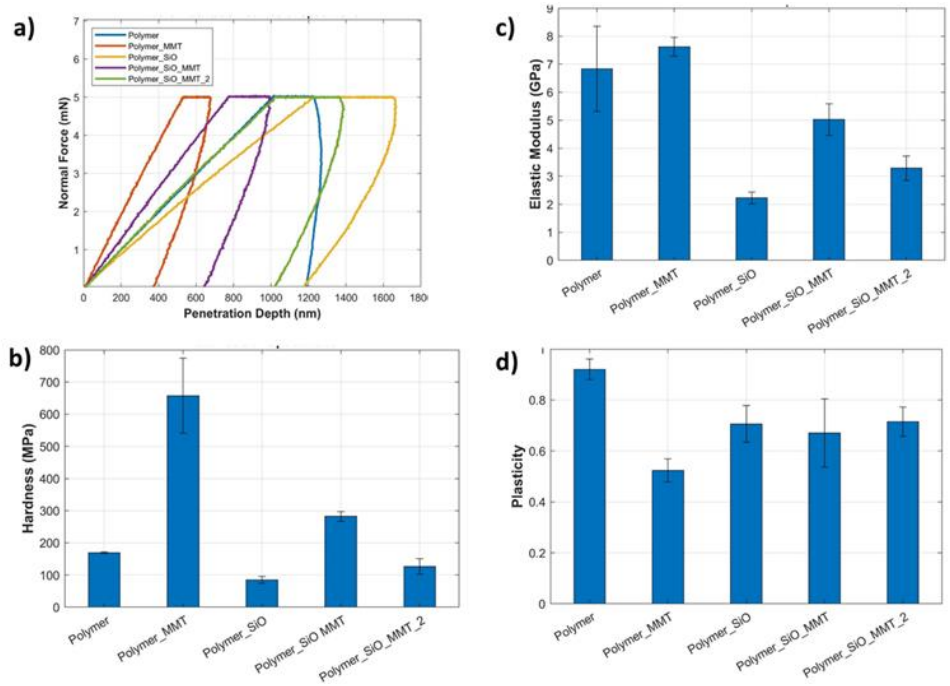

Figure 5. The results of micro-indentation test is shown; a) Representative Penetration Depth-Normal Force curves; b, c, and d represent Elastic Modulus, Hardness and Plasticity values of the specimens.

The plasticity was calculated by the ratio of the plastic work to the total work of force-indentation depth curves which is represented in Figure 6. The ratio of area under unloading curve to the area under loading curve indicates elastic part of work as it is suggested in the previous studies [19– 22] (Equation 3). The calculation was accomplished by numerical integration (multi-step trapezoidal method) and the creep segment of the curves were neglected.

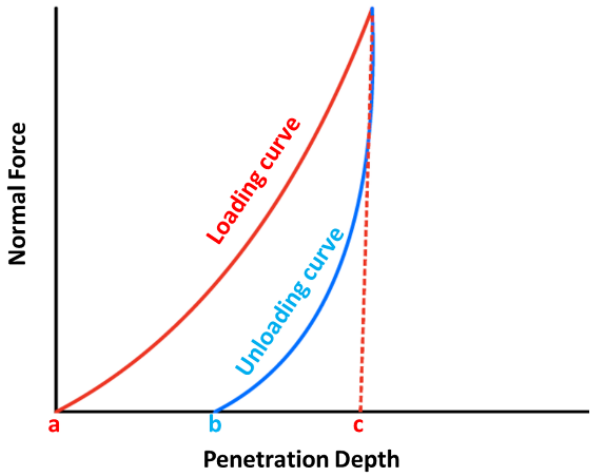

Figure 6. Plasticity was calculated by the ratio of area between the points of (a-b) to the area under loading curve (a-c).

$$Plasticity = \left[1 - \frac{Area\ under\ unloading\ curve}{Area\ under\ loading\ curve}\right] \quad (3)$$

It is seen that the polymer has rather high plasticity (90%) which means that the deformation is mostly unrecoverable when the polymer is unloaded which might be due to the highly cross-linked nature of the polymer. Being a glassy polymer the matrix of this study; NOA 61 is capable of plastic deformations explained by the recent studies. The broadly accepted mechanism consists of two steps [23]. Firstly, 'plasticity carrier polymer chains' are nucleated by the action of the applied load. Secondly, these nucleated plasticity carriers arrange themselves into local ordered-molecular structures which eventually form the macro scaled-plasticity carriers. This phenomenon is analogous to plastic deformation (such as by dislocations) in crystalline solids.

Insertion of 1 wt% MMT (Polymer_MMT) drastically improved the hardness by 288% (Table 2, Figure 5). In fact, the highest improvement in hardness was achieved by this particular nanocomposite. This points out efficient stress transfer from the matrix to reinforcement thanks to both high surface area of MMT and the compatibility between polymer matrix and organic modification of MMT. This is confirmed by both the intercalated/exfoliated silicate layers observed in XRD (Figure 2) and peaks of chemical attractions indicated by FTIR (Figure 4, 5). Elastic modulus of this particular nanocomposite is found to be similar to pristine polymer. Nevertheless, plasticity of the matrix was drastically reduced by 43%. This would occur because the movement of trapped polymer chains between silicate layers might be inhibited. Since this movement could be necessary to form 'local ordered-molecular structures' analogous to dislocations in metals, the blocked movement would reduce the percentage of plastic deformation.

Table 2. The results of the micro-indentation test

	Polymer	**Polymer_MMT**	**Polymer_SiO**	**Polymer_SiO_ MMT**	**Polymer_SiO_M MT_2**
Hardness (MPa)	169.608±2.190	657.394±116.394	84.618±11.015	282.166±15.00	126.906±23.705
Elastic Modulus (GPa)	6.834±1.314	7.613±0.337	2.225±0.213	5.022±0.567	3.288±0.432
Plasticity	0.918±0.035	0.524±0.072	0.706±0.045	0.671±0.134	0.715±0.057

Addition of 1 wt% SiO_2 led to decrease of both hardness and elastic modulus by 51% and 61%, respectively. There should be two reasons for that; firstly, the surface of unmodified-SiO_2 may not be compatible with the polymer matrix as there is no indicative peaks on FTIR curves (Figure 3, 4). Secondly, being a micro-scaled reinforcement, the total surface area of this particular reinforcement is not enough for efficient load transfer. It is well known that concentration of the micro-scaled particles should be optimum for efficient load transfer without leading to agglomeration. It is seen that SiO_2 particles rather act as stress concentration cites diminishing both strength and modulus. However, the plasticity reduction by SiO_2 additive is 21% lower than the reduction observed in Polymer_MMT. It is revealed that in polymer matrix, the surface compatibility of MMT is higher than SiO_2 which is confirmed by both FTIR and XRD (Figure 2, 4). Therefore, due to the loose bond between SiO_2 and the matrix, arrangement of polymer chains into plasticity carriers could become easier.

There seems to be no synergism for hardness and modulus when equal amounts of MMT and SiO_2 added together. The properties falls between the values obtained by the single addition of either MMT or SiO_2 such that simultaneous addition of SiO_2 and MMT changed hardness by -25% and +66% for the composites of Polymer_SiO_MMT_2 and Polymer_SiO_MMT, respectively. This might point out that neither SiO_2 contribution disturb intercalated/exfoliated-MMT structure, nor by simultaneous MMT reinforcement, quality of SiO_2 dispersion is affected. This suggestion is also supported by the preserved exfoliated nature of XRD curves for the SiO_2/MMT mixtures (Figure 2).

It should be noted that one benefit of these SiO_2/MMT combinations over single MMT reinforcement could be related to plasticity since they result in less plasticity reduction (-22% and -27% for Polymer_SiO_MMT_2 and Polymer_SiO_MMT, respectively). In addition to it, their contribution to hardness is higher than bare SiO_2 addition (Table 1). In the study of Fox-Rabinovich et al. [24], plasticity is proved to be contributed to wear resistance of inorganic coatings. This could also be applied to our study as the abrasive wear resistance of organic coatings could be calculated from hardness to elastic modulus ratio. This ratio, according to Fox-Rabinovich et al [24], is analogous to inverse of ratio of elastic work to total work of deformation which is proportional to the plasticity (Equation 4). Therefore, for the applications necessitating wear resistance, Polymer_SiO_MMT could be considered since this particular composite increases hardness of polymer by 66% with relatively small plasticity reduction (-27%).

$$Wear\ Resistance \approx \left[\frac{Area\ under\ unloading\ curve}{Area\ under\ loading\ curve}\right]^{-1} \tag{4}$$

5. CONCLUSION

The outcomes of this study reveal that, on the one hand, 1 wt% addition of MMT resulted in the highest hardness improvement (288%). This behavior is attributed to the intercalated/ exfoliated silicate layers which is confirmed by XRD. The particular peaks in FTIR spectrum also showed the compatibility of surface modification of MMT with the polymer. On the other hand, 1 wt% addition of SiO_2 diminished both the hardness and elastic modulus of the matrix, pointing out the inefficient load transfer from the matrix to the additive. The diminished mechanical properties stem from incompatibility between the surface of the composite constituents and the relatively lower surface area of micro-scaled SiO_2.

In the case of crosslinking density, FTIR spectra show that the addition of either additive leads to the same characteristic peaks of the polymer matrix, which could be interpreted as crosslinking density and adhesion quality were not affected.

Reinforcement by 1 wt% MMT and 1 wt% SiO_2 leads to lower hardness improvement (66%) than bare 1 wt% MMT addition (288%). Nevertheless, this combination resulted in 18% more plasticity than 1 wt% MMT, which could benefit wear resistance.

ACKNOWLEDGEMENTS

This study is funded by TED University Institutional Research Fund under grant number T-18-B2010-33018.

CONFLICT OF INTEREST

The authors stated that there are no conflicts of interest regarding the publication of this article.

REFERENCES

[1] Ahmad KZK, Ahmad SH, Tarawneh MA & Apte PR. Evaluation of Mechanical Properties of Epoxy / Nanoclay / Multi-Walled Carbon Nanotube Nanocomposites using Taguchi Method, 2012; 4: 80–86.

[2] Ahmad T & Mamat O. Studying the Effects of Adding Silica Sand Nanoparticles on Epoxy Based Composites. J Nanoparticle 2013.

[3] Alsagayar ZS, Rahmat AR, Arsad A & Mus SNHB. Tensile and Flexural Properties of Montmorillonite Nanoclay Reinforced Tensile and Flexural Properties of Montmorillonite Nanoclay Reinforced Epoxy Resin Composites. Adv Mat Res 2015; 1112: 373–376.

[4] Briscoe, BJ., Fiori, L, & Pelillo. Nano-indentation of polymeric surfaces. J Phys D Appl Phys, 1998; 31(19): 2395–2405.

[5] Donmez F, Kandemir AC & Kaplan CH. Biocompatible nanocomposite production via nanoclays with diverse morphology. Int J Polym Anal Charact 2022; 27 (13): 158-179.

[6] Bufford D, Liu Y, Wang J, Wang H & Zhang X. In situ nanoindentation study on plasticity and work hardening in aluminium with incoherent twin boundaries. Nat Commun 2014; 5.

[7] Castriota M, Fasanella A, Cazzanelli E, De Sio L, Caputo R & Umeton C. In situ polarized micro-Raman investigation of periodic structures realized in liquid-crystalline composite materials. Optics Express 2011; 19(11):10494.

[8] De Menezes LR & Da Silva EO. The use of montmorillonite clays as reinforcing fillers for dental adhesives. Mater Res 2016; 19(1): 236–242.

[9] Díez-Pascual AM, Gómez-Fatou, MA, Ania F & Flores A. Nanoindentation in polymer nanocomposites. Prog Mater Sci 2015; 67:1-95.

[10] Encalada-Alayola JJ, Veranes-Pantoja Y, Uribe-Calderón JA, Cauich-Rodríguez JV & Cervantes-Uc JM. Effect of type and concentration of nanoclay on the mechanical and physicochemical properties of bis-GMA/TTEGDMA dental resins. Polym 2020; 12(3)

[11] Fox-Rabinovich GS, Veldhuis SC, Scvortsov VN, Shuster LS, Dosbaeva GK & Migranov MS. Elastic and plastic work of indentation as a characteristic of wear behavior for cutting tools with nitride PVD coatings. Thin Solid Films 2004; 469(2): 505–512.

[12] Gerberich WW, Stauffer DD, Beaber AR & Mook WM. Connectivity between plasticity and brittle fracture: An overview from nanoindentation studies. Proceedings of the Institution of Mechanical Engineers, Part N: Journal of Nanoengineering and Nanosystems, 2007; 221(4): 139–156.

[13] Kandemir, AC, Erdem D, Ma H, Reiser A & Spolenak R. Polymer nanocomposite patterning by dip-pen nanolithography. Nanotechnology 2016; 27 (13):135303

[14] Kandemir AC, Ramakrishna SN, Erdem D, Courty D, & Spolenak R. Gradient nanocomposite printing by dip pen nanolithography. Comp Sci Tech 2017; 138: 186–200.

[15] Lam CK, Lau KT & Zhou LM. Nano-mechanical Creep Properties of Nanoclay / Epoxy Composite by Nanoindentation. Adv Comp Mater Struct 2007; 335: 669–672.

[16] Li Y, Li C, He J, Gao Y, & Hu Z. Effect of functionalized nano-SiO2 addition on bond behavior of adhesively bonded CFRP-steel double-lap joint. Constr Build Mater 2020; 244:118400

[17] Ma Z, Jiang D, Cui Y & Liu Y. The Development of Nanoclay-Epoxy Composite for Application in Ballistic Protection , SAE Technical Papers, 2018

[18] Meng Q, Wang CH, Saber N, Kuan H, Dai J, Friedrich K & Ma J. Nanosilica-toughened polymer adhesives. Mater Des, 2014; 61: 75–86.

[19] Milman YV, Chugunova SI & Goncharova IV. Plasticity determined by indentation and theoretical plasticity of materials. Bulletin of the Russian Academy of Sciences: Physics, 2009; 73(9):1215–1221.

[20] Milman YV, Chugunova SI, Goncharov IV & Golubenko AA. Plasticity of materials determined by the indentation method. Prog Phys Metals 2008; 19(3): 271-308

[21] Nai MH, Lim CT, Zeng KY & Tan VBC. Nanoindentation study of polymer based nanocomposites. J Metastable Nanocryst Mater 2005; 23: 363–366

[22] Norland Products Incorporated. (1966). Norland Optical Adhesives 61 Datasheet.

[23] Oleinik EF, Mazo MA, Strel'nikov IA, Rudnev SN & Salamatina OB. Plasticity Mechanism for Glassy Polymers: Computer Simulation Picture. Polym Sci - Series A. 2018; 60(1): 1-49

[24] Yasin S, Shakeel A, Iqbal T, Ahmad F, Mehmood H, Luckham PF & Ullah N. Effect of experimental conditions on nano-indentation response of low density polyethylene (LDPE). J Macromol Sci 2019; 56(7), 640–647.

[25] Oliver WC & Pharr GM. An Improved Technique for Determining Hardness and Elastic Modulus Using Load and Displacement Sensing Indentation Experiments. J Mater Res 1992; 7(6): 1564–1583.

[26] Oliver WC and Pharr GM. Measurement of Hardness and Elastic Modulus by Instrumented Indentation: Advances in Understanding and Refinements to Methodology. J Mater Res 2004; 19(01): 3–20.